



## Extracting Information from the Power Spectrum of Synaptic Noise

ALAIN DESTEXHE\* AND MICHAEL RUDOLPH

*Integrative and Computational Neuroscience Unit (UNIC), CNRS, 91198 Gif-sur-Yvette, France*

Destexhe@iaf.cnrs-gif.fr

*Received April 7, 2004; Revised June 26, 2004; Accepted July 12, 2004*

Action Editor: Xiao-Jing Wang

**Abstract.** In cortical neurons, synaptic “noise” is caused by the nearly random release of thousands of synapses. Few methods are presently available to analyze synaptic noise and deduce properties of the underlying synaptic inputs. We focus here on the power spectral density (PSD) of several models of synaptic noise. We examine different classes of analytically solvable kinetic models for synaptic currents, such as the “delta kinetic models,” which use Dirac delta functions to represent the activation of the ion channel. We first show that, for this class of kinetic models, one can obtain an analytic expression for the PSD of the total synaptic conductance and derive equivalent stochastic models with only a few variables. This yields a method for constraining models of synaptic currents by analyzing voltage-clamp recordings of synaptic noise. Second, we show that a similar approach can be followed for the PSD of the membrane potential ( $V_m$ ) through an effective-leak approximation. Third, we show that this approach is also valid for inputs distributed in dendrites. In this case, the frequency scaling of the  $V_m$  PSD is preserved, suggesting that this approach may be applied to intracellular recordings of real neurons. In conclusion, using simple mathematical tools, we show that  $V_m$  recordings can be used to constrain kinetic models of synaptic currents, as well as to estimate equivalent stochastic models. This approach, therefore, provides a direct link between intracellular recordings *in vivo* and the design of models consistent with the dynamics and spectral structure of synaptic noise.

**Keywords:** synaptic noise, computational models, power spectrum, cerebral cortex

### Introduction

Because of the relatively high levels of activity of cortical neurons in active states (1–20 Hz sustained firing; Evarts, 1964; Steriade, 1978; Matsumura et al., 1988; Steriade et al., 2001), combined with their high interconnectivity (Cragg, 1967; Szentagothai, 1965; DeFelipe and Fariñas, 1992; DeFelipe et al., 2002), cortical neurons usually display intense synaptic background activity, also called “synaptic noise.” Synaptic noise can have a significant impact on the integrative properties of cortical neurons, as suggested by dynamic-clamp experiments and computational models (reviewed in Destexhe et al., 2003). However, be-

cause of the highly complex nature of these membrane potential ( $V_m$ ) fluctuations, few methods are presently available to analyze synaptic noise and deduce properties of the underlying synaptic inputs.

Different approaches have been used to model synaptic noise. Biophysical models explicitly considered thousands of synapses that generate synaptic noise, in single-compartment neurons (Lánský and Rodriguez, 1999; Tiesinga et al., 2000; Tuckwell et al., 2002), as well as in models incorporating dendritic morphology (Bernander et al., 1991; Rapp et al., 1992; Destexhe and Paré, 1999; Rudolph and Destexhe, 2003a). Another approach is based on a “diffusion approximation” and consists of modeling synaptic noise by a stochastic process in which noise is added to the membrane (Johannesma, 1968; Ricciardi 1976;

\*To whom correspondence should be addressed.

Hanson and Tuckwell, 1983; Lánský and Lánská, 1987; Lánský and Rospars, 1995; Doiron et al., 2000; Brunel et al., 2001; van Rossum, 2001). In order to account for the high-conductance state induced by synaptic noise, an intermediate approach was proposed and modeled synaptic noise as arising from stochastic processes applied to two conductances (excitatory and inhibitory), each described by a separate stochastic process (Destexhe et al., 2001). This type of model can be used in dynamic-clamp experiments, and recreates active states *in vitro* (Destexhe et al., 2001; Chance et al., 2002; Fellous et al., 2003; Prescott and De Koninck, 2003; Rudolph et al., 2004). Although this approach can successfully reproduce the modulating features of synaptic noise, there is presently no available method to adjust this type of model to experimental data.

We focus here on different classes of analytically-solvable kinetic models for synaptic currents, such as the “delta kinetic models” which use Dirac delta functions to represent the activation of the ion channel. This approximation is justified by the fact that the binding of the transmitter occurs on a very fast time scale compared to the state transitions and decay kinetics of postsynaptic channels. The transmitter reaches relatively high concentrations in the synaptic cleft, but this increase of concentration is very brief (reviewed in Clements, 1996). The opening of the channel is then driven by this very fast event, while the closing time is governed by the slower rate constants of the transitions between open and closed states.

We show here that, under this approximation, the kinetics of the channel is solvable exactly, even with multiple states. In the case of postsynaptic channels, delta kinetic models provide computationally efficient algorithms to handle synaptic interactions (see also Destexhe et al., 1994). In this case, the analytic solution enables us to calculate exactly the power spectral density (PSD) of synaptic conductances, and under some approximation, the PSD of the  $V_m$ , similar to previous studies (Manwani and Koch, 1999). The goal of this approach is to provide a link between experimentally-observed PSDs of synaptic noise and the kinetics of the underlying conductances, in order to build simplified models that preserve their spectral structure.

## Methods

We consider here models of synaptic noise and its power spectral density (PSD), which were simulated by three approaches. The simplest approach was to

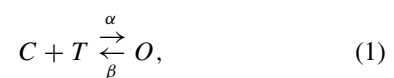
simulate a single-compartment model including two stochastic conductances (Destexhe et al., 2001). Different models were used to simulate the stochastic conductances, and these models are detailed below (see Results). An intermediate approach was to simulate a single-compartment model with a large number of individual synapses releasing randomly (Rudolph et al., 2004). Finally, models based on three-dimensional reconstructions of cortical neurons were used and were taken from a previous study (Destexhe and Paré, 1999). In the two latter cases, different kinetic models were considered for synaptic conductances, and correspond to different schemes of the activation of postsynaptic receptors (see details in Results). Finally, Fourier transform were calculated numerically either from conductances or from the voltage, using standard algorithms (Press et al., 1986). All models and calculations were done using the NEURON simulator (Hines and Carnevale, 1997).

## Results

We start by considering the simplest elementary kinetic scheme for modeling synaptic conductances, then we turn to more complex models in the following sections. For each model, we derive the power spectral density (PSD) of synaptic noise, as well as the best simplified model matching this PSD. In the last section, we focus on synaptic noise at the level of the membrane potential ( $V_m$ ), and derive analytic approximations for its PSD.

### *Two-State Kinetic Models and “Exponential Synapses”*

The simplest model of postsynaptic receptors consists of a two-state scheme of the binding of transmitter ( $T$ ) to the closed form of the channel ( $C$ ), leading to its open form ( $O$ ):



where  $\alpha$  and  $\beta$  are the forward and backward rate constants, respectively. In most cases, these rate constants are independent of voltage, although they are voltage-dependent for some receptor types (e.g., NMDA receptors). We will only consider voltage-independent rate constants in the present study.

The corresponding kinetic equation for this scheme is:

$$\frac{dc}{dt} = \alpha T (1 - c) - \beta c, \quad (2)$$

where  $c$  is the fraction of channels in the open state. The synaptic current is given by:

$$I_{\text{syn}}(t) = g_{\text{max}} c(t) (V - E_{\text{syn}}), \quad (3)$$

where  $g_{\text{max}}$  is the maximal conductance of the synapse,  $V$  is the membrane potential, and  $E_{\text{syn}}$  is the reversal potential of the conductance.  $c(t)$  denotes the fraction of channels in the open state, such that  $g_{\text{max}} c(t)$  is the synaptic conductance at time  $t$ .

The release and clearance of transmitter are extremely fast phenomena compared to open/close channel kinetics, resulting in a very brief presence of transmitter in the synaptic cleft (Clements, 1996). For the sake of simplicity, we restrict here to a class of models in which the transmitter time course is modeled as a Dirac delta function  $\delta(t - t_j)$  occurring at the times of presynaptic spikes ( $t_j$ ). Applying this to the two-state scheme above yields the following kinetic equation:

$$\frac{dc}{dt} = \alpha(1 - c) \sum_j \delta(t - t_j) - \beta c, \quad (4)$$

where the sum runs over all presynaptic spikes  $j$ .

This equation is solvable by Fourier or Laplace transform. The Fourier transform of Eq. (4) reads:

$$C(\omega) = \frac{\alpha \sum_j [1 - c(t_j)] e^{-i\omega t_j}}{\beta + i\omega}, \quad (5)$$

where  $\omega = 2\pi f$  is the angular frequency,  $f$  is the frequency, and  $C(\omega)$  is the Fourier transform of  $c(t)$ . Assuming uncorrelated inputs, this expression leads to the following power spectral density (PSD) for  $c$ :

$$P_c(\omega) = |C(\omega)|^2 = \frac{\alpha^2 \sum_j [1 - c(t_j)]^2}{\beta^2 + \omega^2}, \quad (6)$$

as well as the explicit solution of  $c(t)$ :

$$c(t) = \alpha \sum_j [1 - c(t_j)] e^{-\beta(t-t_j)}. \quad (7)$$

Thus, the delta-pulse activation of the channels at each time  $t_j$  leads to an instantaneous rise of  $c$ , by an amount depending on the state of  $c$  at that time,  $[1 - c(t_j)]$ , followed by an exponential decay at a rate

$\beta$ . This summing behavior is illustrated in Fig. 1A, where successive conductance increases depend on the previous activation state of the receptor. This model, therefore, implements *saturating exponential synaptic currents* because the amplitude of each exponent is modulated by the state of the channel (term  $[1 - c(t_j)]$ ).

One particular case worth considering is when the closed form  $C$  is always in excess compared to the open form  $O$ , then all terms in  $(1 - c) \simeq 1$ . The kinetic equation becomes:

$$\frac{dc}{dt} = \alpha \sum_j \delta(t - t_j) - \beta c, \quad (8)$$

with the PSD for  $c$ :

$$P_c(\omega) = \frac{\alpha^2 \lambda}{\beta^2 + \omega^2}, \quad (9)$$

where  $\lambda$  is the average rate of presynaptic spikes, and the explicit solution is:

$$c(t) = \alpha \sum_j e^{-\beta(t-t_j)}. \quad (10)$$

In this case, as illustrated in Fig. 1B, we have a summation of identical exponential waveforms, consisting of an instantaneous rise of  $\alpha$  at each time  $t_j$ , followed by an exponential decay. In contrast to the saturating model (Fig. 1A), there is no dependence on the prior activation state of the channel. This *exponential synaptic current* model is widely used to represent synaptic interactions (Dayan and Abbott, 2001; Gerstner and Kistler, 2002).

#### *Equivalence with an Ornstein-Uhlenbeck Process for Random Inputs*

We now examine the case of exponential synapses submitted to a high-frequency train of random presynaptic inputs. If the synaptic conductance time course is the same for each event (e.g., nonsaturating exponential synapse, Eq. (8) above), and if successive events are triggered according to a Poisson-process, then the conductance of the synapse can be described by a *shot noise process*. In this case, for high enough presynaptic average frequency, it can be demonstrated that the synaptic conductance  $g$  will approach a Gaussian distribution (Papoulis, 1991), which is characterized by its mean  $g_0$  and standard deviation  $\sigma_g$ . These values are given by using Campbell's theorem (Campbell, 1909;

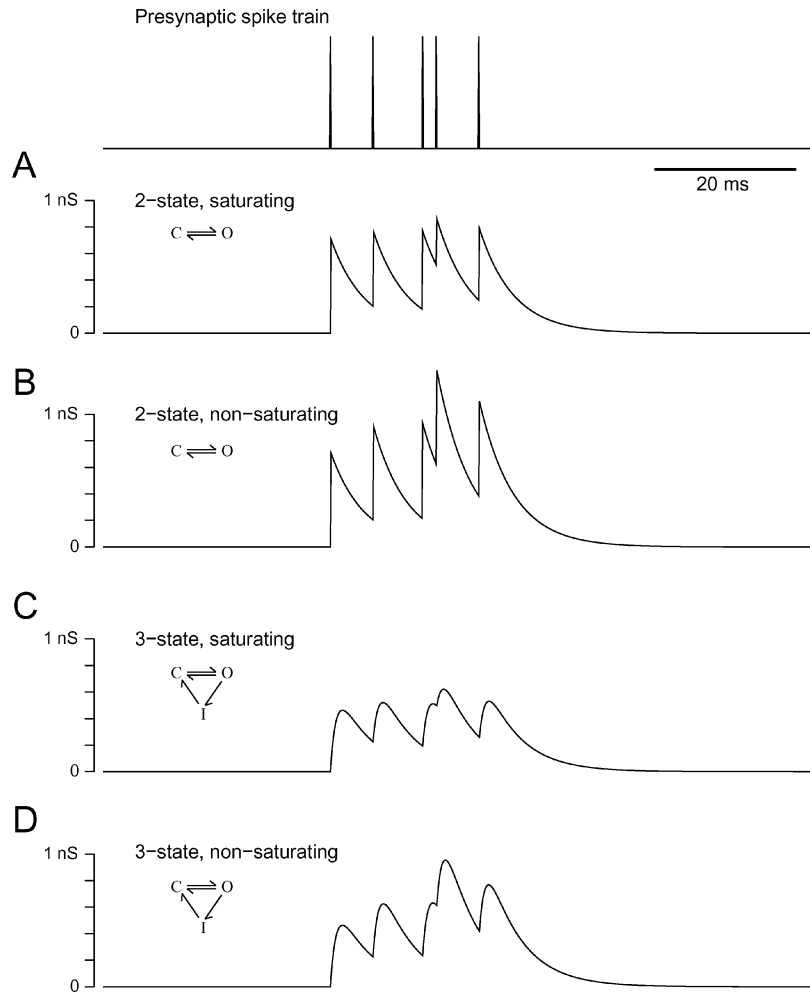


*Figure 1.* Summating synaptic conductances in different models of fast glutamatergic currents. Following the same presynaptic pattern of spikes (top), different models of postsynaptic glutamate (AMPA) receptors, activated by Dirac delta functions, are compared. A. 2-state kinetic model with saturation (Eq. (4);  $\alpha = 0.72 \text{ ms}^{-1}$ ,  $\beta = 0.21 \text{ ms}^{-1}$ ,  $g_{\max} = 1 \text{ nS}$ ). B. 2-state kinetic model without saturation (Eq. (8); same parameters as in A). C. 3-state kinetic model with saturation (Eqs. (18) and (19);  $\alpha = 0.72 \text{ ms}^{-1}$ ,  $\beta = 0.1 \text{ ms}^{-1}$ ,  $\gamma = 1.155 \text{ ms}^{-1}$ ,  $\varepsilon = 0.21 \text{ ms}^{-1}$ ). D. 3-state kinetic model without saturation (Eqs. (25) and (26); same parameters as in C). In all cases, the numerical simulation of the differential equations is superimposed to the explicit analytic solution of the same equations (the traces are indistinguishable). See text for details.

Papoulis, 1991): for a shot-noise process of rate  $\lambda$  and described by:

$$s(t) = \sum_j p(t - t_j), \quad (11)$$

where  $p(t)$  is the time course of each event occurring at time  $t_j$ , the average value  $s_0$  and variance  $\sigma_s$  are given by:

$$s_0 = \lambda \int_{-\infty}^{\infty} p(t) dt, \quad \sigma_s^2 = \lambda \int_{-\infty}^{\infty} p^2(t) dt. \quad (12)$$

Applying this theorem to the conductance of exponential synapses, we have:

$$\int_{-\infty}^{\infty} g(t) dt = \int_{-\infty}^{\infty} g_{\max} \alpha e^{-\beta t} dt = \frac{g_{\max} \alpha}{\beta},$$

which combined with Eq. (12) gives the following expressions for the mean and variance of the synaptic conductance:

$$g_0 = \frac{\lambda g_{\max} \alpha}{\beta}, \quad \sigma_g^2 = \frac{\lambda g_{\max}^2 \alpha^2}{2\beta}. \quad (13)$$

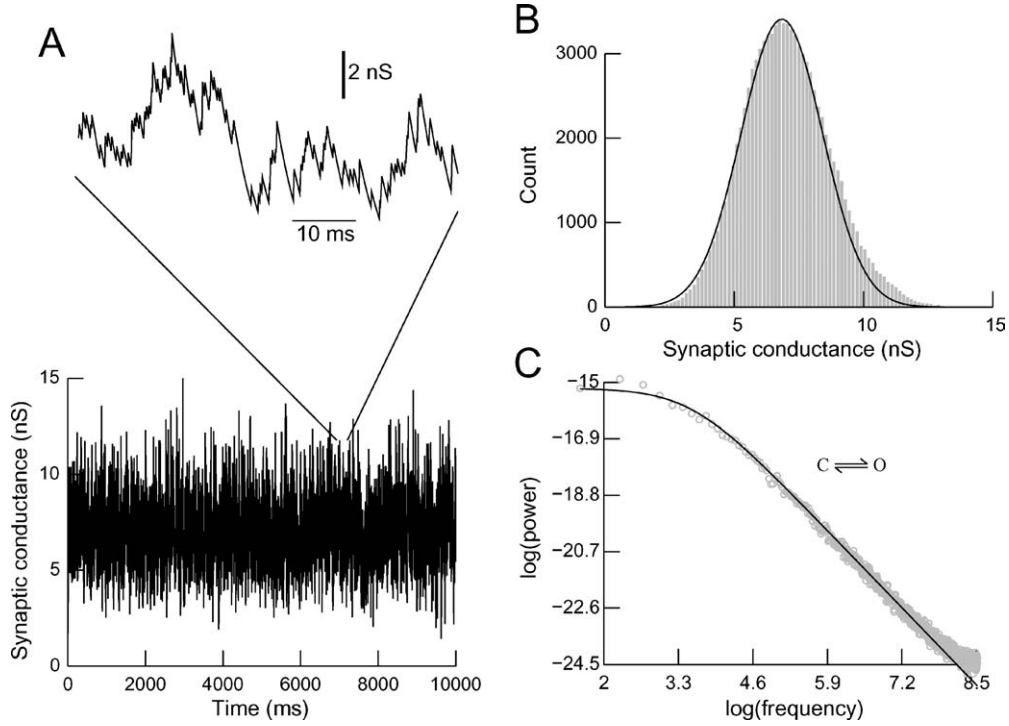


**Figure 2.** Random synaptic inputs using two-state kinetic models. A. Synaptic conductance resulting from high-frequency random stimulation of the nonsaturating exponential synapse model (Eq. (8);  $\alpha = 0.72 \text{ ms}^{-1}$ ,  $\beta = 0.21 \text{ ms}^{-1}$ ,  $g_{\max} = 1 \text{ nS}$ ). Presynaptic inputs were Poisson-distributed (average rate of  $\lambda = 2000 \text{ s}^{-1}$ ). The conductance time course (bottom; inset at higher magnification on top) shows the irregular behavior resulting from these random inputs. B. Distribution of conductance. The histogram (gray) was computed from the model shown in A (bin size of  $0.15 \text{ nS}$ ). The conductance distribution is asymmetric, although well approximated by a Gaussian (black), with mean and variance calculated from Campbell's theorem (see Eqs. (12) and (13)). C. Power spectrum of the conductance. The power spectral density (PSD, represented here in log-log scale) was calculated from the numerical simulations of the model in A (circles) and was compared to the theoretical value of the PSD of an Ornstein-Uhlenbeck stochastic process (black; see text for details).

Thus, for a large number of synaptic inputs triggered by a Poisson process, the mean and variance of the conductance distribution can be estimated from Campbell's theorem. Figure 2 illustrates this behavior by simulating numerically an exponential synapse triggered by a high-frequency Poisson process (Fig. 2A). The distribution of the conductance is asymmetric (Fig. 2B, histogram), although close to a Gaussian (Fig. 2B, continuous curve). This Gaussian curve was obtained using the mean and the variance estimated from Eq. (13), which provide a good approximation of the conductance distribution.

We can compare this shot-noise process to the following Gaussian stochastic process:

$$\frac{dg}{dt} = -(g - g_0)/\tau + \sqrt{D} \chi(t), \quad (14)$$

where  $g = g_{\max}c$ ,  $D$  is the amplitude of the stochastic component,  $\chi(t)$  is a normally-distributed (zero-mean) noise source, and  $\tau$  is the time constant ( $\tau = 0$  gives white noise,  $\tau > 0$  yields "colored" noise). This process is similar to a well-known model of Brownian motion (Uhlenbeck and Ornstein, 1930), and has been used to model the stochastic variations of synaptic conductances *in vivo* (Destexhe et al., 2001). It is also Gaussian-distributed, with a mean value of  $g_0$  and a variance given by  $\sigma_g^2 = D\tau/2$ .

To relate these two models, we use the expression of the PSD of the Ornstein-Uhlenbeck process:

$$P_g(\omega) = \frac{2D\tau^2}{1 + \omega^2\tau^2}. \quad (15)$$

This Lorentzian form is equivalent to Eq. (9), from which we can deduce that  $\tau = 1/\beta$ . The relation

$\sigma_g^2 = D\tau/2$ , combined with Eq. (13), gives the expression for the amplitude of the noise:

$$D = \lambda g_{\max}^2 \alpha^2. \quad (16)$$

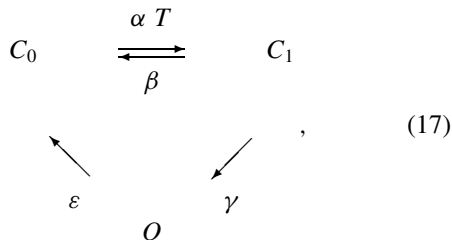
Using these expressions, the predicted PSD matches very well the numerical simulations of Poisson-distributed synaptic currents described by 2-state kinetic models, as illustrated in Fig. 2C.

Thus, we can conclude that the model of nonsaturating exponential synaptic currents, Eq. (8) is very well described by an Ornstein-Uhlenbeck process in the case of a large number of random inputs. The decay time of the synaptic current gives the ‘‘correlation time’’ ( $\tau$ ) of the noise, whereas the other parameters of the Ornstein-Uhlenbeck process can be deduced directly from the parameters of the kinetic model of the synaptic conductance.

*Three-State Kinetic Models and ‘‘Biexponential Synapses’’*

The equivalence presented above shows that modeling synaptic ‘‘noise’’ by an Ornstein-Uhlenbeck process on the conductances (as in Destexhe et al., 2001) implicitly assumes that all synaptic events are described by identical, instantaneously rising and exponential decaying synaptic events. The possible influence of the more complex form of synaptic currents is neglected in this case. In order to evaluate the impact of such a simplification, we consider now more complex models of synaptic currents that include a finite rise time, such as three-state models (see below), arbitrarily complex Markov kinetic schemes (see Appendix 2), or pulse-based kinetic models (see Appendix 3).

The following three-state kinetic scheme was introduced for modeling postsynaptic receptors (Destexhe et al., 1994):



where  $C_0$  and  $C_1$  are the closed forms of the receptor,  $O$  is the open (conducting) form, and  $\alpha$ ,  $\beta$ ,  $\gamma$  and  $\varepsilon$  are voltage-independent rate constants. Making the

following delta-pulse assumptions as above, the kinetic equations for this system are:

$$\frac{dc}{dt} = \alpha (1 - c - r) \sum_j \delta(t - t_j) - (\beta + \gamma) c, \quad (18)$$

$$\frac{dr}{dt} = \gamma c - \varepsilon r, \quad (19)$$

where  $c$  and  $r$  represent the fraction of receptors in forms  $C_1$  and  $O$ , respectively, and the sum runs over all presynaptic spikes  $j$ . As for Eq. (4), this equation is solvable by Fourier or Laplace transform. The Fourier transform of  $c$  is similar to Eq. (6) above; (Eq. (18) is almost identical to Eq. (4)), while the transform of  $r$  reads:

$$\begin{aligned}
 R(\omega) &= \frac{\alpha\gamma}{(\beta + \gamma + i\omega)(\varepsilon + i\omega)} \\
 &\times \sum_j [1 - c(t_j) - r(t_j)] e^{-i\omega t_j}, \quad (20)
 \end{aligned}$$

from which we can deduce the PSD of  $r$ :

$$P_r(\omega) = |R(\omega)|^2 = \frac{\alpha^2\gamma^2 \sum_j [1 - c(t_j) - r(t_j)]^2}{[(\beta + \gamma)^2 + \omega^2] [\varepsilon^2 + \omega^2]}, \quad (21)$$

as well as its explicit solution:

$$\begin{aligned}
 r(t) &= \frac{\alpha\gamma}{\beta + \gamma - \varepsilon} \sum_j [1 - c(t_j) - r(t_j)] \\
 &\times [e^{-\varepsilon(t-t_j)} - e^{-(\beta+\gamma)(t-t_j)}]. \quad (22)
 \end{aligned}$$

In this case, the delta-pulse activation of the channels at each time  $t_j$  leads to a biexponential solution, in which the conductance rises with a fast time constant, equal to  $\tau_1 = 1/(\beta + \gamma)$ , and decays exponentially with a time constant of  $\tau_2 = 1/\varepsilon$ . This biexponential time course is modulated by the availability of channels in the closed state at the time of each spike,  $[1 - c(t_j) - r(t_j)]$ , as illustrated in Fig. 1C. This model, therefore, implements *saturating biexponential synaptic currents* and is a generalization of the exponential synaptic mechanism examined in the previous section.

Two cases are worth considering. First, let us consider the case where the two time constants are equal

( $\tau_1 = \tau_2 = \tau$ ). In such a case, the transform of  $r$  reads:

$$R(\omega) = \frac{\alpha\gamma}{(1/\tau + i\omega)^2} \sum_j [1 - c(t_j) - r(t_j)] e^{-i\omega t_j}, \quad (23)$$

which explicit solution is:

$$r(t) = \alpha\gamma \sum_j [1 - c(t_j) - r(t_j)] (t - t_j) e^{-(t-t_j)/\tau}. \quad (24)$$

Thus, in this case, the solution of the 3-state scheme gives rise to a functional form similar to an alpha-function,  $t \exp(-t/\tau)$ , with an additional mechanism for saturation through the dependence on the availability of closed channels (term  $[1 - c(t_j) - r(t_j)]$ ). This particular case with  $\tau_1 = \tau_2$  can, therefore, be used to model *saturating alpha synaptic currents*.

Another special case to consider is, as in the case of the two-state kinetic model, when the closed form  $c$  is always in excess compared to the other forms, then all terms in  $(1 - c - r) \simeq 1$ . The kinetic equations then become:

$$\frac{dc}{dt} = \alpha \sum_j \delta(t - t_j) - (\beta + \gamma) c, \quad (25)$$

$$\frac{dr}{dt} = \gamma c - \varepsilon r, \quad (26)$$

which yields the following PSD for  $r$ :

$$P_r(\omega) = \frac{\alpha^2 \gamma^2 \lambda}{[(\beta + \gamma)^2 + \omega^2] [\varepsilon^2 + \omega^2]}, \quad (27)$$

as well as the following explicit solution for  $r$ :

$$r(t) = \frac{\alpha\gamma}{\beta + \gamma - \varepsilon} \sum_j [e^{-\varepsilon(t-t_j)} - e^{-(\beta+\gamma)(t-t_j)}]. \quad (28)$$

In this case, as illustrated in Fig. 1D, we have a summation of identical biexponential waveforms, each characterized with stereotyped amplitude, rising and decay time constants. This *biexponential synaptic current* model is also widely used to represent synaptic interactions (Koch, 1999).

As above, one can further simplify Eq. (22) by setting  $\tau_1 = \tau_2 = \tau$ , which yields:

$$r(t) = \alpha\gamma \sum_j (t - t_j) e^{-(t-t_j)/\tau}. \quad (29)$$

This expression consists of *summed alpha functions* and is also a model that was used in many theoretical studies (e.g., Manwani and Koch, 1999).

Note that a frequency scaling in  $\omega^{-4}$  for the PSD can also be obtained from models based on single exponentials. In its simplest version, the “pulse-based kinetic model” (Destexhe et al., 1994) consists of a two-state kinetic scheme, Eq. (1), in which  $T$  occurs as a pulse of fixed amplitude and duration. During the pulse, the synaptic conductance increases exponentially, then after the pulse, it decays back to zero with a single exponential time course (Fig. 3A, left; see Appendix 3 for equations). The PSD of this type of model is more complex than above (see Appendix 3), but shows an asymptotic scaling behavior that depends on the model parameters (Fig. 3). For the reference parameters (i.e., those obtained by fitting this model to experiments; see Destexhe et al., 1994), the PSD shows oscillations due to the discontinuous derivative of the conductance (see Lowen and Teich, 1990) and asymptotically scales as  $\omega^{-4}$  (Fig. 3A, right). As expected, when the rising phase of the pulse is very sharp, this model tends to Eq. (4), and in this case, the PSD scales as  $\omega^{-2}$  (Fig. 3B). Interestingly, for intermediate values, the asymptotic scaling can be intermediate between  $\omega^{-2}$  and  $\omega^{-4}$  (Fig. 3C). Indeed, one can show that this model initially scales as a Lorentzian ( $\omega^{-2}$ ), then scales in  $\omega^{-4}$  for high frequencies (see Appendix 3 for details).

#### *Equivalent Ornstein-Uhlenbeck Type Process for Biexponential Synapses*

In the case of a large number of Poisson-distributed random synaptic inputs described by biexponential synapses, if we use the nonsaturating model, Eqs. (25) and (26), then we have a shot noise process. In such a case, using Campbell’s theorem, Eq. (12), the mean and variance of the conductance are given by:

$$g_0 = \frac{\lambda g_{\max} \alpha \gamma}{\varepsilon(\beta + \gamma)}, \quad \sigma_g^2 = \frac{\lambda g_{\max}^2 \alpha^2 \gamma^2}{2\varepsilon(\beta + \gamma)(\beta + \gamma - \varepsilon)}. \quad (30)$$

The numerical simulation of such a process is illustrated in Fig. 4A. As in the case of exponential inputs, the conductance distribution is asymmetric (Fig. 4B, histogram), and is in relatively good agreement with the Gaussian distribution predicted by the values given above in Eq. (30) (Fig. 4B, black).

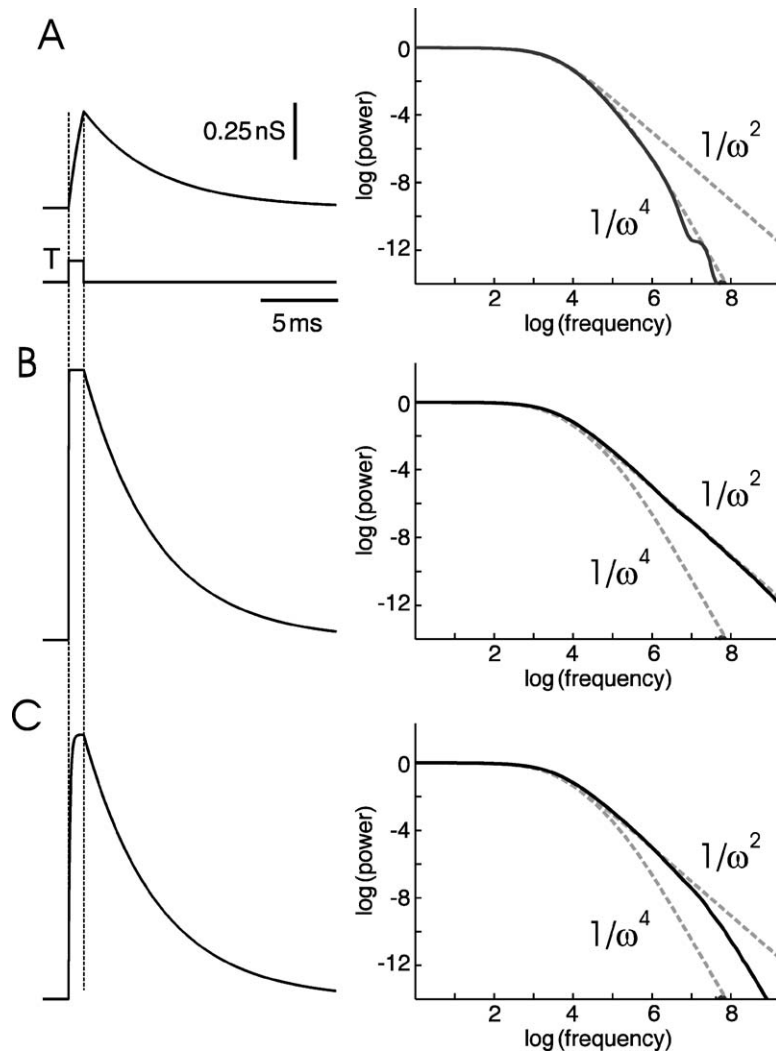


*Figure 3.* Power spectral density of pulse-based kinetic models of synaptic currents. A. Pulse-based kinetic model of AMPA synaptic currents using parameters estimated from fitting the model to experimental data ( $T_{\text{dur}} = 1$  ms,  $T_{\text{max}} = 1$  mM,  $\alpha = 0.5$  ms $^{-1}$  mM $^{-1}$ ,  $\beta = 0.23$  ms $^{-1}$ ; see Destexhe et al., 1994). B. Pulse-based kinetic model with very sharp rising phase (same parameters except  $\alpha = 100$  ms $^{-1}$  mM $^{-1}$ ). C. Pulse-based kinetic model with intermediate rising phase (same parameters except  $\alpha = 10$  ms $^{-1}$  mM $^{-1}$ ). In all cases the left panels show an example of an isolated synaptic event, and the right panels display the PSD (in log-log scale) obtained from the conductance resulting from a large number of randomly releasing synapses. The dashed lines indicate scaling in  $\omega^{-2}$  (two-state delta kinetic model) and  $\omega^{-4}$  (three-state delta kinetic model) for comparison. The PSD of pulse-based models can show a frequency scaling consistent with either type (A, B), or intermediate (C).

Because their power spectra do not scale as a Lorentzian (see (Eq. (27))), biexponential synapses cannot be adequately represented by the Ornstein-Uhlenbeck process, Eq. (14). However, one can generalize this process to the case of biexponential synapses. Noting that the kinetic equation for  $c$ , Eq. (25), is of identical form as the simple exponential synapse, Eq. (8),  $c$  can therefore be described by an Ornstein-Uhlenbeck process similar to Eq. (14), but this process must be augmented by an equation to describe

the additional variable  $r$ . This leads to the following two-variable stochastic process:

$$\begin{aligned} \frac{dC}{dt} &= -(C - C_0)/\tau_1 + \sqrt{D} \chi(t), \\ \frac{dg}{dt} &= \gamma C - g/\tau_2, \end{aligned} \quad (31)$$

where  $g = g_{\text{max}} r$ ,  $C = g_{\text{max}} c$ , and  $\tau_1$  and  $\tau_2$  are the associated time constants. The PSD of this stochastic

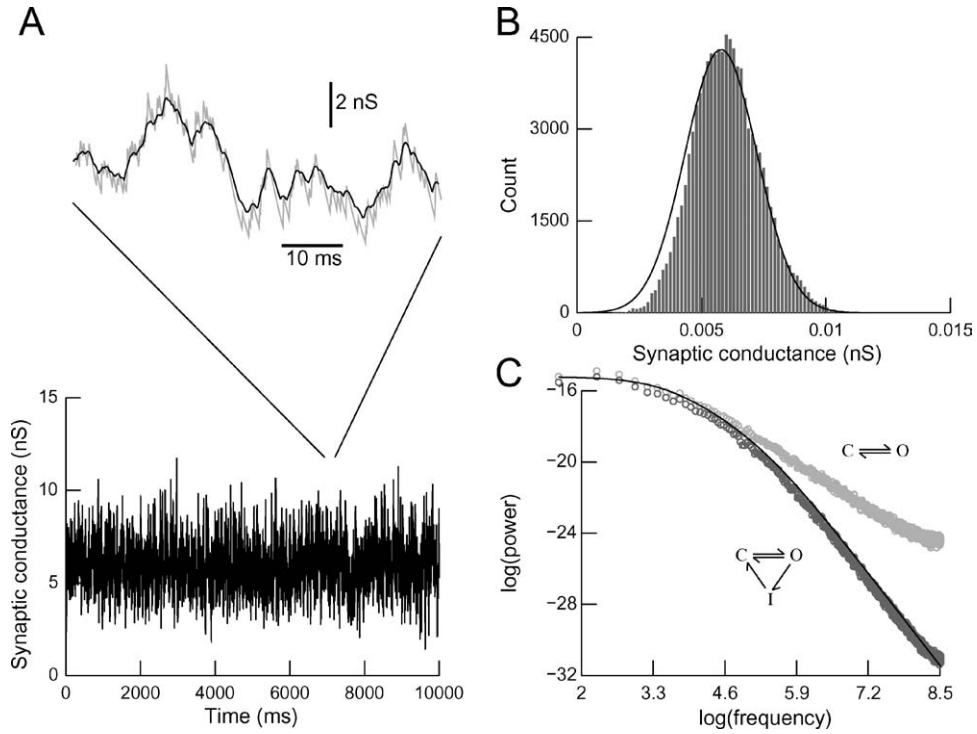


**Figure 4.** Random synaptic inputs using three-state kinetic models. A. Synaptic conductance resulting from high-frequency random stimulation of the nonsaturating biexponential synapse model (Eqs. (25) and (26);  $\alpha = 0.72 \text{ ms}^{-1}$ ,  $\beta = 0.1 \text{ ms}^{-1}$ ,  $\gamma = 1.155 \text{ ms}^{-1}$ ,  $\varepsilon = 0.21 \text{ ms}^{-1}$ ,  $g_{\max} = 1 \text{ nS}$ ). Presynaptic inputs were Poisson-distributed (average rate of  $\lambda = 2000 \text{ s}^{-1}$ ). The inset on top shows the conductance at a higher magnification (black), overlaid with the conductance obtained with the 2-state kinetic model (light gray; model from Fig. 2A, inset; the same random numbers were used in both models). B. Distribution of conductance. The histogram (dark gray) was computed from the model shown in A (bin size of 0.15 nS). The conductance distribution is asymmetric, although well approximated by a Gaussian (black line), with mean and variance calculated from Campbell's theorem (see Eq. (30)). C. Power spectrum of the conductance. The power spectral density (PSD, in log-log scale) was calculated from the numerical simulations of the model in A (dark gray circles) and was compared to the theoretical value of the PSD of an extended Ornstein-Uhlenbeck stochastic process (black; scaling in  $\omega^{-4}$ ). The PSD of the 2-state model (light gray circles; from Fig. 2C) is shown for comparison (scaling in  $\omega^{-2}$ ).

process is given by:

$$P_g(\omega) = \frac{2D\gamma^2\tau_1^2\tau_2^2}{(1 + \omega^2\tau_1^2)(1 + \omega^2\tau_2^2)}. \quad (32)$$

This form is equivalent to Eq. (27), from which one can recover  $\tau_1 = 1/(\beta + \gamma)$  and  $\tau_2 = 1/\varepsilon$ . Similarly as above, the amplitude of the noise is given by:

$$D = \lambda g_{\max}^2 \alpha^2. \quad (33)$$

The power spectrum predicted using these relations (Fig. 4C, line) matches very well the numerical simulations of random synaptic inputs using three-state kinetic models (Fig. 4C, dark grey circles). On the other hand, there is a qualitative difference in the power spectra obtained using two- and three-state kinetic models

(light and dark grey circles in Fig. 4C), suggesting that the calculation of the PSD of experimentally recorded conductances should yield important constraints on the underlying kinetic model.

#### Membrane Potential Fluctuations

We have shown above that under some assumptions, one can obtain analytic estimates of the power spectra of synaptic conductances which could in principle be used to analyze experimental data. However, these estimates are only applicable to voltage-clamp experiments. Most experiments (in particular, *in vivo* recordings) are performed in current-clamp mode, in which case the membrane potential activity is recorded. One therefore needs methods to extract the characteristics

of the synaptic inputs under current-clamp by analyzing the voltage fluctuations, which is the subject of this section.

Assuming a passive isopotential cell, the time evolution of the voltage is given by:

$$C_m \frac{dV}{dt} = -g_{\text{leak}} (V - E_{\text{leak}}) - \sum_j g_j(t) (V - E_{\text{syn}}), \quad (34)$$

where  $V$  is the membrane potential,  $C_m = 1 \mu\text{F}/\text{cm}^2$  is the specific membrane capacitance,  $g_{\text{leak}} = 0.1 \text{ mS}/\text{cm}^2$  and  $E_{\text{leak}} = -70 \text{ mV}$  are the leak conductance and reversal potential, respectively. The membrane is subject to a large number of conductance-based synaptic inputs,  $g_j(t)$ , with corresponding reversal potential  $E_{\text{syn}}$ .

Taking the Fourier transform of the membrane equation yields:

$$i\omega C_m V(\omega) = -g_{\text{leak}} [V(\omega) - E_{\text{leak}}\delta(\omega)] - \sum_j g_j(\omega) * [V(\omega) - E_{\text{syn}}], \quad (35)$$

where  $*$  is the convolution operator. This equation is not solvable, precisely because of this convolution, which is a consequence of the multiplicative aspect of conductances.

To solve this equation, we make an “effective leak approximation” (e.g., Brunel and Wang, 2001; Rudolph and Destexhe, 2003b). This approximation is justified by the fact that in high-conductance states, it was estimated that the total membrane conductance is always about 2 orders of magnitude larger than the conductance of single synapses (Destexhe and Paré, 1999). In this case, the voltage deflection due to isolated inputs is small compared to the distance to reversal potential, and we can consider the driving force as approximately constant. However, we must take into account the high-conductance state of the membrane, which is the sum of all average membrane conductances. The membrane equation then becomes:

$$C_m \frac{dV}{dt} = -g_T (V - \bar{V}) - \sum_j (g_j(t) - \bar{g}_j)(\bar{V} - E_{\text{syn}}), \quad (36)$$

where  $\bar{g}_j$  is the average conductance at each synapse,  $g_T = g_{\text{leak}} + \sum_j \bar{g}_j$  is the total average membrane conductance, and  $\bar{V}$  is the average membrane potential. Note that the driving force ( $\bar{V} - E_{\text{syn}}$ ) is now

constant, which is therefore equivalent to approximate conductance-based inputs as current-based inputs, but arising on top of a large overall membrane conductance.

Taking the Fourier transform, one obtains, for  $\omega > 0$ :

$$V(\omega) = \frac{\sum_j g_j(\omega)(E_{\text{syn}} - \bar{V})}{g_T + i\omega C_m}. \quad (37)$$

The PSD is then given by:

$$P_V(\omega) = |V(\omega)|^2 = \frac{|\sum_j g_j(\omega)(E_{\text{syn}} - \bar{V})|^2}{g_T^2 + \omega^2 C_m^2}. \quad (38)$$

If all synaptic inputs are based on the same quantal events, then  $g_j(\omega) = g(\omega)$ , and incorporating the “effective” membrane time constant  $\tilde{\tau}_m = C_m/g_T$ , we can write:

$$P_V(\omega) = \frac{C |g(\omega)|^2}{1 + \omega^2 \tilde{\tau}_m^2}, \quad (39)$$

where  $C = \lambda (E_{\text{syn}} - \bar{V})^2 / g_T^2$ .

Thus, the PSD of the membrane potential is here expressed as a “filtered” version of the PSDs of synaptic conductances, where the filter is given by the RC circuit of the membrane in the high-conductance state. Taking the example of two-state kinetic synapses, Eq. (4), the PSD of the membrane potential is given by:

$$P_V(\omega) = \frac{C'}{(1 + \omega^2 \tau_{\text{syn}}^2)(1 + \omega^2 \tilde{\tau}_m^2)}, \quad (40)$$

where  $\tau_{\text{syn}} = 1/\beta$  and  $C' = g_{\text{max}}^2 \alpha^2 C \beta^2$ . This expression was tested numerically for a model receiving thousands of random conductance-based synaptic inputs (Fig. 5A). For models receiving only excitatory synapses (Fig. 5B), or only inhibitory synapses (Fig. 5C), the prediction provided by Eq. (40) (black curves) was in excellent agreement with the numerical simulations (circles). When both excitatory and inhibitory inputs were present (Fig. 5D), the theoretical PSD was obtained by a sum of two expressions similar to Eq. (40), and still was in excellent agreement with the numerical simulations.

In the case of three-state kinetic models, Eqs. (18) and (19), the PSD is given by:

$$|V(\omega)|^2 = \frac{C''}{(1 + \omega^2 \tau_1^2)(1 + \omega^2 \tau_2^2)(1 + \omega^2 \tilde{\tau}_m^2)}, \quad (41)$$

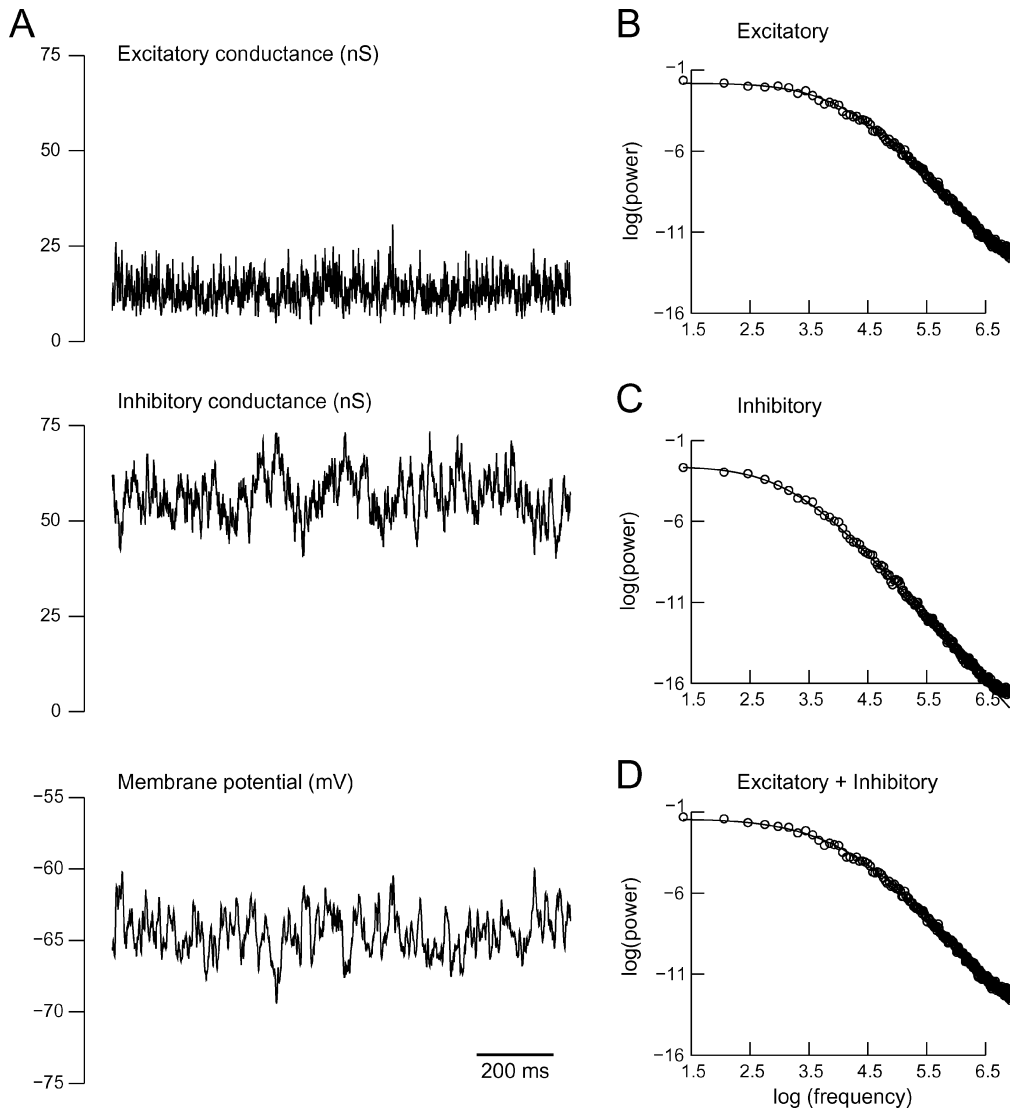


**Figure 5.** Power spectral estimates of the membrane potential in a model with random synaptic inputs. A. Simulation of a single-compartment neuron receiving a large number of randomly releasing synapses (4470 AMPA-mediated and 3800 GABA<sub>A</sub>-mediated synapses, releasing according to independent Poisson processes of average rate of 2.2 and 2.4 Hz, respectively). The total excitatory (AMPA) conductance, the total inhibitory (GABA<sub>A</sub>) conductance and the membrane potential are shown from top to bottom in the first second of the simulation. B. Power spectral density (PSD) calculated for a model with only excitatory synapses (inhibitory synapses were replaced by a constant equivalent conductance of 56 nS). C. PSD calculated for a model with only inhibitory synapses (excitatory synapses were replaced by a constant equivalent conductance of 13 nS). D. PSD calculated for the model shown in A, in which both excitatory and inhibitory synapses participated to membrane potential fluctuations. In B–D, the continuous curves show the theoretical prediction from Eq. (40). All synaptic inputs were equal (quantum of 1.2 nS for AMPA and 0.6 nS for GABA<sub>A</sub>) and were described by two-state kinetic models.

where  $\tau_1 = 1/(\beta + \gamma)$  and  $\tau_2 = 1/\varepsilon$  are the time constants associated with the three-state kinetic model, and  $C'' = g_{\max}^2 \alpha^2 \gamma^2 C / [(\beta + \gamma)^2 \varepsilon^2]$ . Simulations of random synaptic inputs using this model yielded slightly different voltage fluctuations compared to the two-state kinetic model (Fig. 6A). This differ-

ence was also apparent in the PSD calculated from the  $V_m$  of both models (Fig. 6B, circles). The analytic estimates of the PSD, Eq. (41), yielded a remarkable agreement with the PSD obtained numerically from the conductance-based model (Fig. 6B, black).

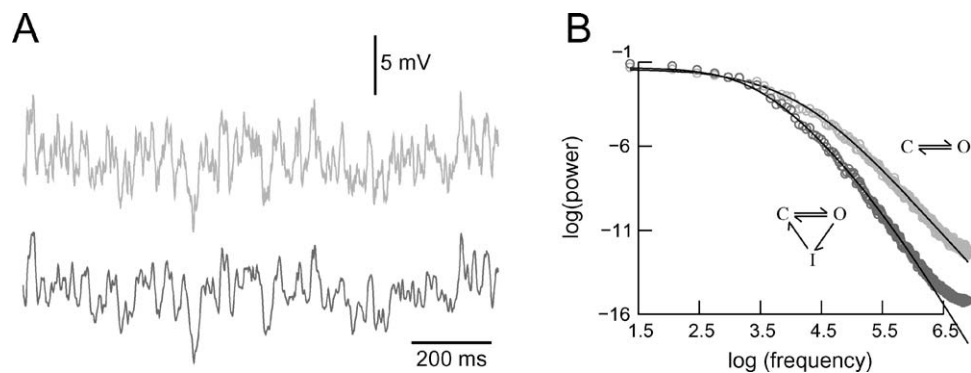


**Figure 6.** Power spectral estimates of the membrane potential for two different kinetic models of synaptic inputs. **A.** Simulation of a single-compartment neuron receiving a large number of randomly releasing synapses, according to two different kinetic models. Light gray: two-state kinetic model (same model as in Fig. 5A); Dark gray: three-state kinetic model (same parameters). In both cases, excitatory and inhibitory synapses participated to membrane potential fluctuations and the same random numbers were used (same parameters as in Fig. 5A). **B.** Power spectral density (PSD) calculated for numerical simulations (light gray circles: two-state model; dark gray circles: three-state model). The continuous curves show the theoretical predictions from Eq. (40) (two-state model) and Eq. (41) (three-state model).

The simulations above clearly show that the PSD of the  $V_m$  can be well predicted theoretically. These expressions can therefore be used in principle to fit the parameters of the kinetic models of synaptic currents from the PSD of the  $V_m$  activity. Not all parameters, however, can be estimated. The reason is that several parameters appear combined (such as in the expression of  $C'$  and  $C''$  above), in which case they cannot be distinguished from the PSD alone. Nevertheless, it is possible to fit the different time constants of the system, as well as the asymptotic scaling behavior at high frequencies.

These considerations are valid only for a single-compartment model, and they may not apply to the case of synaptic inputs distributed in dendrites. Because of the strong low-pass filtering properties of dendrites, it is possible that distributed synaptic inputs would affect the scaling behavior of the PSD of the  $V_m$ . To investigate this point, we used a previously published model of synaptic background activity *in vivo* (Destexhe and Paré, 1999), and calculated the PSD of the  $V_m$  in a high-conductance state due to the random release of excitatory and inhibitory synapses distributed in soma and dendrites (Fig. 7, circles). This PSD was

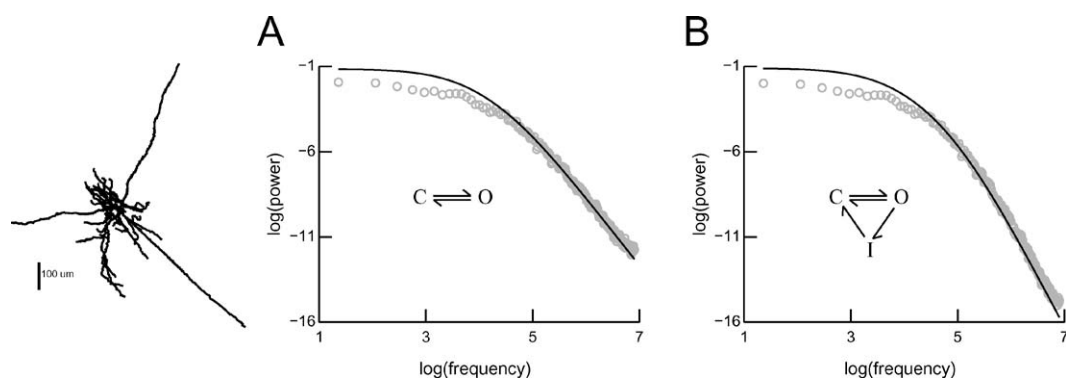


**Figure 7.** Power spectrum of models with synaptic inputs distributed in dendrites. Simulations of a passive compartmental model of cat layer VI pyramidal neuron (left) receiving a large number of randomly-releasing synapses (16563 AMPA-mediated and 3376 GABA<sub>A</sub>-mediated synapses, releasing according to independent Poisson processes of average rate of 1 and 5.5 Hz, respectively). This model simulates the release conditions during high-conductance states *in vivo* (see details in Destexhe and Paré, 1999). **A.** Power spectrum obtained for the somatic  $V_m$  in this model when synaptic inputs were simulated by two-state kinetic models (gray circles). The continuous curve shows the theoretical PSD of the  $V_m$  obtained in an equivalent single-compartment model. **B.** Same simulation and procedure, but using three-state (biexponential) synapse models. In both cases, the decay of the PSD at high frequencies was little affected by dendritic filtering.

compared to the theoretical expressions obtained above for a single-compartment model with equivalent synaptic inputs (Fig. 7, continuous lines). Surprisingly, there was little effect of dendritic filtering on the frequency scaling of the PSD of the  $V_m$ . In particular, the scaling at large frequencies was minimally affected (compare continuous lines with circles in Fig. 7). These simulations, therefore, suggest that the spectral structure of synaptic noise, as seen from the  $V_m$ , could provide a reliable method to yield information about the underlying synaptic inputs.

## Discussion

Using simple mathematical tools, we have focused here on two of the main classes of functions used to represent synaptic conductances, namely the “exponential synapses,” which consist of an instantaneous rise followed by exponential decay, and the “biexponential synapses,” in which the rise and decay are controlled by a double exponential form with two time constants. These two classes respectively correspond to two-state and three-state kinetic models, in which the transmitter activation is represented by a Dirac delta function. These “delta kinetic models” are very convenient, because they can be manipulated analytically without invoking complex mathematical frameworks, which leads to a number of useful expressions, as discussed below.

First, the synaptic conductance can be obtained analytically for arbitrarily complex input streams, similar to pulse-based kinetic models (Destexhe et al., 1994) or event-based algorithms (Mattia and Del Giudice, 2000). This is valid both for exponential and biexponential synapses, as well as for their variants, such as saturating or nonsaturating alpha functions. As a result, there is no need to solve differential equations for the synaptic inputs, which results in the possibility of designing fast algorithms for computing synaptic interactions (see details in Appendix 1). In principle, this approach should apply to more complex Markov kinetic models (see Appendix 2).

Second, for the case of a large number of random synaptic inputs, we have shown a procedure to obtain the closest stochastic process to describe the total synaptic conductance. For the simplest type of exponential synapses, the total conductance can be described by a Gaussian (Fig. 2B), and has a power spectrum scaling like a Lorentzian (Fig. 2C). These features are typical of the Ornstein-Uhlenbeck stochastic

process (Uhlenbeck and Ornstein, 1930). This model is, therefore, an extremely good approximation for a large number of synaptic inputs of this kind, although there is no formal equivalence between these two processes (e.g., the third and fourth moments are non zero, as deduced by Campbell’s theorem). For three-state kinetic models, the biexponential synaptic conductances lead to a PSD that significantly departs from a Lorentzian (Fig. 4C) and cannot be described by the Ornstein-Uhlenbeck process. We have introduced an extended two-variable Ornstein-Uhlenbeck stochastic process which matches the statistical and spectral properties of the biexponential synapses (Fig. 4). Here again, the approach should apply to arbitrarily complex Markov kinetic schemes described by delta kinetic models. The corresponding stochastic process to model global conductances would be  $n$ -dimensional generalizations of the Ornstein-Uhlenbeck process.

Finally, we examined the PSD of the membrane potential for neurons subject to conductance-based synaptic inputs. In this case, the PSD of the  $V_m$  is not accessible because of the nonlinearity of conductances. However, we showed that in high-conductance states, this PSD is very well approximated by that of a current-based model, but only if the total conductance of the membrane is taken into account. This effective leak approximation (for other related approaches, see Manwani and Koch, 1999; Brunel and Wang, 2001) allowed us to predict the frequency dependence of the PSD of  $V_m$  activity. Remarkably, the frequency scaling was little affected in the case of synaptic inputs distributed in dendrites, suggesting that this method may be used as a tool for analyzing experimental data. For example, the frequency dependence of the  $V_m$  activity could be used to find which is the simplest kinetic model to describe the experiments, a task which would be very difficult *in vivo* because of the impossibility to observe isolated synaptic events. Using the procedure detailed above, one can also find the closest Ornstein-Uhlenbeck type process to reproduce synaptic noise with the correct spectral structure. Because the latter models are very fast to simulate, they are readily applicable to dynamic-clamp experiments to “recreate” active states *in vitro* (Destexhe et al., 2001; Chance et al., 2002; Fellous et al., 2003; Prescott and De Koninck, 2003; Rudolph et al., 2004). The present computational approach therefore provides a direct link between intracellular recordings *in vivo* and the design of precise and efficient models of synaptic noise for being used *in vitro*.

### Appendix 1: Algorithms for Simulating Multiple Synaptic Inputs

In the case of  $N$  synapses described by the 2-state kinetic model, Eq. (8), if these synapses converge on the same postsynaptic compartment, we have:

$$I_{\text{syn}}(t) = g_{\text{max}} G(t) (V - E_{\text{syn}}), \quad (42)$$

where  $G(t) = \sum_{k=1}^N c_k(t)$  is the sum over the state variables  $c_k$  of all synapses. Each state variable is described by:

$$\frac{dc_k}{dt} = \alpha \sum_j \delta(t - t_j^k) - \beta c_k, \quad (43)$$

where  $t_j^k$  is the  $j$ th spike arriving at synapse  $k$ .

Summing over this equation, leads to:

$$\frac{dG}{dt} = \alpha \sum_{j,k} \delta(t - t_j^k) - \beta G, \quad (44)$$

which is functionally identical to Eq. (8) and, therefore, has the following explicit solution:

$$G(t) = \alpha \sum_{j,k} e^{-\beta(t-t_j^k)}. \quad (45)$$

Thus, multiple synapses can be handled by a single “multi-synapse” mechanism in which all presynaptic spikes are merged into a unique presynaptic train. This approach is similar to the analytic treatment of discrete voltage jumps which form the basis of event-based algorithms (Mattia and Del Giudice, 2000).

In the case of saturating exponential synapses, Eq. (4), each state variable is described by:

$$\frac{dc_k}{dt} = \alpha(1 - c_k) \sum_j \delta(t - t_j^k) - \beta c_k, \quad (46)$$

which, after summation, yields:

$$\frac{dG}{dt} = \alpha \sum_{j,k} (1 - c_k) \delta(t - t_j^k) - \beta G. \quad (47)$$

The explicit solution is given by:

$$G(t) = \alpha \sum_{j,k} [1 - c_k(t_{j-1}^k)] e^{-\beta(t-t_j^k)}. \quad (48)$$

This case is more complex, because the state variable of individual synapses ( $c_k$ ) still appears. This type of multi-synapse mechanism must therefore keep track of

the state variable of each synapse at the time of the corresponding spike,  $c_k(t_j^k)$ . This can easily be calculated from the state variable at the time of the preceding spike,  $c_k(t_{j-1}^k)$ , by using the expression:

$$c_k(t_j^k) = \alpha [1 - c_k(t_{j-1}^k)] e^{-\beta(t_j^k - t_{j-1}^k)}. \quad (49)$$

In the case of the 3-state kinetic model, Eqs. (25) and (26), a set of  $N$  synapses are also described by Eq. (42), but in this case  $G(t) = \sum_{k=1}^N r_k(t)$ , where  $r_k$  is the fraction of receptors in the open state for each synapse. Using the same notations as above, the time evolution of the state variables of each synapse is given by:

$$\frac{dc_k}{dt} = \alpha \sum_j \delta(t - t_j^k) - (\beta + \gamma) c_k, \quad (50)$$

$$\frac{dr_k}{dt} = \gamma c_k - \varepsilon r_k. \quad (51)$$

Summing over these two equations leads to:

$$\frac{dF}{dt} = \alpha \sum_{j,k} \delta(t - t_j^k) - (\beta + \gamma) F, \quad (52)$$

$$\frac{dG}{dt} = \gamma F - \varepsilon G, \quad (53)$$

where  $F(t) = \sum_{k=1}^N c_k(t)$ . The explicit solution of this system is given by:

$$G(t) = \frac{\alpha\gamma}{\beta + \gamma - \varepsilon} \sum_{j,k} [e^{-\varepsilon(t-t_j^k)} - e^{-(\beta+\gamma)(t-t_j^k)}]. \quad (54)$$

For saturating biexponential synapses, Eqs. (18) and (19), similar considerations lead to the following explicit solution for the multisynapse:

$$G(t) = \frac{\alpha\gamma}{\beta + \gamma - \varepsilon} \sum_{j,k} [1 - c_k(t_{j-1}^k) - r_k(t_{j-1}^k)] \times [e^{-\varepsilon(t-t_j^k)} - e^{-(\beta+\gamma)(t-t_j^k)}], \quad (55)$$

where the values of the state variables are given by:

$$c_k(t_j^k) = \alpha [1 - c_k(t_{j-1}^k) - r_k(t_{j-1}^k)] e^{-(\beta+\gamma)(t_j^k - t_{j-1}^k)}, \quad (56)$$

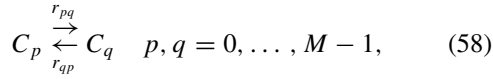
$$r_k(t_j^k) = \frac{\alpha\gamma}{\beta + \gamma - \varepsilon} [1 - c_k(t_{j-1}^k) - r_k(t_{j-1}^k)] \times [e^{-\varepsilon(t_j^k - t_{j-1}^k)} - e^{-(\beta+\gamma)(t_j^k - t_{j-1}^k)}]. \quad (57)$$

Thus,  $N$  synapses described by either 2-state or 3-state kinetics can be merged into one multi-synapse

handling all the presynaptic spikes. The explicit solutions given above for  $G(t)$  can be used to directly calculate the conductance of the ensemble of  $N$  synapses, without solving any differential equation, thus resulting in computationally efficient algorithms.

## Appendix 2: General Solution for Markov Kinetic Models

Consider a ligand-gated ion channel with  $M$  states  $C_k$ ,  $k = 0, \dots, M-1$ , where  $C_0$  denotes the closed state and  $C_{M-1}$  the open state of the channel. These states obey the following set of transitions:



where  $\{r_{pq}\}$  are the rate constants associated with all possible transitions between two states. One or several of these states can be conducting. In the analysis below, all transitions are permitted to stay general, except for transitions from any state to itself, for which  $r_{pp} = 0$ ,  $p = 0, \dots, M-1$ . If a transition does not occur, the corresponding rate constant will be set to zero. For transitions that involve the binding of transmitter, the rate constant will be written as:

$$r_{pq} = \bar{r}_{qp} \sum_j \delta(t - t_j). \quad (59)$$

This formulation is generic and accounts for most Markov kinetic diagrams introduced to model ligand-gated ion channels. In particular, the three-state diagram in Eq. (17) can be obtained by setting  $M = 2$ ,  $C_2 = O$ ,  $\bar{r}_{01} = \alpha$ ,  $r_{10} = \beta$ ,  $r_{12} = \gamma$ ,  $r_{20} = \varepsilon$ , and the other rates to zero.

This generic state diagram is described by the following set of  $M$  kinetic equations:

$$\frac{dc_k(t)}{dt} = \sum_{\substack{i=0 \\ i \neq k}}^{M-1} r_{ik}(t)c_i(t) - \sum_{\substack{i=0 \\ i \neq k}}^{M-1} r_{ki}(t)c_k(t) \quad k = 0, \dots, M-1 \quad (60)$$

and

$$1 = \sum_{k=0}^{M-1} c_k(t). \quad (61)$$

This system of  $(M+1)$  equations describes the time course of  $M$  variables  $c_k(t)$ ,  $k = 0, \dots, M-1$ , subject

to the constraining relation given in Eq. (61). The latter can be used to eliminate one of the differential equations, thus yielding the system of  $(M-1)$  equations

$$\frac{dc_k(t)}{dt} = r_{0k}(t) \left( 1 - \sum_{i=1}^{M-1} c_i(t) \right) + \sum_{\substack{i=1 \\ i \neq k}}^{M-1} r_{ik}(t)c_i(t) - \sum_{\substack{i=0 \\ i \neq k}}^{M-1} r_{ki}(t)c_k(t), \quad (62)$$

$k = 1, \dots, M-1$ , which describes the time evolution of the fraction of channels in states  $C_k$ ,  $k > 0$ . Before restricting to specific cases of transmitter release, we will investigate below the general  $M$ -state kinetic model and its solution.

Due to the, so far, unconstrained time- and voltage-dependence of the rate constants  $r_{kl}(t)$ , a general explicit solution of the system given in Eq. (62) can not be written down. To allow access, we assume the voltage-independence of  $r_{kl}(t)$ . Furthermore, without loss of generality, we assume that transmitter binding transitions only occur from the closed state  $C_0$  to the  $k$ th state  $C_k$ ,  $k = 1, \dots, M-1$  with rates  $r_{0k}(t) = \alpha_k T_k(t)$ , where  $\alpha_k$  are time-independent rate constants and  $T_k(t)$  denotes the arbitrary time-course of transmitter release for the corresponding transition. All other rate constants are time-independent, i.e.,  $r_{kl}(t) = \beta_{kl}$ . With these assumptions, Eq. (62) reads:

$$\frac{dc_k(t)}{dt} = \alpha_k T_k(t) \left( 1 - \sum_{i=1}^{M-1} c_i(t) \right) + \sum_{\substack{i=1 \\ i \neq k}}^{M-1} \beta_{ik} c_i(t) - \sum_{\substack{i=0 \\ i \neq k}}^{M-1} \beta_{ki} c_k(t) \quad (63)$$

with  $k = 1, \dots, M-1$ .

This system of coupled first-order linear differential equations can be solved by Fourier transform. Defining

$$c_k(t) = \frac{1}{2\pi} \int_{-\infty}^{\infty} d\omega C_k(\omega) e^{i\omega t}, \quad (64a)$$

$$T_k(t) = \frac{1}{2\pi} \int_{-\infty}^{\infty} d\omega T_k(\omega) e^{i\omega t}, \quad (64b)$$

where  $\omega = 2\pi f$  is the angular frequency,  $f$  is the frequency, and  $C_k(\omega)$  and  $T_k(\omega)$  denote the Fourier transforms of  $c_k(t)$  and  $T_k(t)$ , respectively. With this, we

obtain for  $k = 1, \dots, M - 1$ :

$$i\omega C_k(\omega) = \alpha_k T_k(\omega) + \sum_{\substack{i=1 \\ i \neq k}}^{M-1} \beta_{ik} C_i(\omega) - \sum_{\substack{i=0 \\ i \neq k}}^{M-1} \beta_{ki} C_k(\omega) - \frac{\alpha_k}{2\pi} \sum_{i=1}^{M-1} \int_{-\infty}^{\infty} d\omega' T_k(\omega - \omega') C_i(\omega'), \quad (65)$$

as a description of the  $M$ -state kinetic model with arbitrary integrable time-course of transmitter release.

Equation (65) can be further simplified by restricting to transmitter release whose time course is described by Dirac's  $\delta$ -function, i.e.  $\delta(t - t_j)$  for a release occurring at the time  $t_j$  of a presynaptic spike. Assuming that this kinetic scheme holds for all transmitter binding transitions, we have:

$$T_k(t) = \sum_j \delta(t - t_j) \quad \forall k, \quad (66)$$

where the sum runs over all presynaptic spikes which trigger a transmitter release. The Fourier transform of  $T_k(t)$  is given by:

$$T_k(\omega) = \sum_j e^{-i\omega t_j} \quad \forall k, \quad (67)$$

which yields:

$$\int_{-\infty}^{\infty} d\omega' T_k(\omega - \omega') C_i(\omega') = 2\pi \sum_j e^{-i\omega t_j} c_i(t_j) \quad \forall k. \quad (68)$$

Using these relations, Eq. (65) can be rewritten in matrix form

$$\mathbf{A}(\omega) \mathbf{C}(\omega) = \mathbf{B}(\omega), \quad (69)$$

with the  $(M - 1) \times (M - 1)$ -matrix

$$\mathbf{A}(\omega) = \begin{pmatrix} i\omega + \sum_{\substack{i=0 \\ i \neq 1}}^{M-1} \beta_{1i} & -\beta_{21} & \cdots & -\beta_{(M-1)1} \\ -\beta_{12} & i\omega + \sum_{\substack{i=0 \\ i \neq 2}}^{M-1} \beta_{2i} & \cdots & -\beta_{(M-1)2} \\ \vdots & \vdots & \ddots & \vdots \\ -\beta_{1(M-1)} & -\beta_{2(M-1)} & \cdots & i\omega + \sum_{\substack{i=0 \\ i \neq M-1}}^{M-1} \beta_{(M-1)i} \end{pmatrix}, \quad (70)$$

the  $(M - 1)$ -vectors

$$\begin{aligned} \mathbf{B}(\omega) &= \sum_j e^{-i\omega t_j} \left( 1 - \sum_{i=1}^{M-1} c_i(t_j) \right) \begin{pmatrix} \alpha_1 \\ \alpha_2 \\ \vdots \\ \alpha_{M-1} \end{pmatrix} \\ &= \sum_j e^{-i\omega t_j} c_0(t_j) \begin{pmatrix} \alpha_1 \\ \alpha_2 \\ \vdots \\ \alpha_{M-1} \end{pmatrix}, \end{aligned} \quad (71)$$

and

$$\mathbf{C}(\omega) = \begin{pmatrix} C_1(\omega) \\ C_2(\omega) \\ \vdots \\ C_{M-1}(\omega) \end{pmatrix}. \quad (72)$$

By applying Cramer's rule, Eq. (69) can be solved, yielding:

$$C_k(\omega) = \frac{a}{A(\omega)} \sum_{i=1}^{M-1} (-1)^{k+i} B_i^\delta(\omega) a_{ik}(\omega) \quad (73)$$

for  $k = 1, \dots, M - 1$ , where  $A(\omega) = \det \mathbf{A}(\omega)$ ,  $B_i(\omega)$  denotes the  $i$ th element of  $\mathbf{B}(\omega)$ , and  $a_{ik}(\omega)$  denotes the minor of element  $A_{ik}(\omega)$  of  $\mathbf{A}(\omega)$ . This provides an explicit solution for  $C_k(\omega)$  if the fraction of channels in the closed state  $C_0$ , i.e.,  $c_0(t_j)$ , is known at the times of presynaptic spikes.

Next, we investigate the  $\omega$ -dependence of the general Fourier transforms Eq. (73). Because  $A(\omega) = \det \mathbf{A}(\omega)$  with  $\mathbf{A}(\omega)$  given by Eq. (70), it is a polynomial of order  $(M - 1)$  in  $(i\omega)$  and can be written in the form:

$$A(\omega) = \sum_{m=0}^{M-1} a_m (i\omega)^m, \quad (74)$$

where the coefficients  $a_m$  are functions of the constant rates  $\beta_{ik}$  only. Equivalently,  $a_{ik}(\omega)$  are the minors of  $\mathbf{A}(\omega)$ , i.e., determinants of some  $(M - 2) \times (M - 2)$ -matrices  $\mathbf{A}'_{ik}(\omega)$ , and, hence, polynomials at most of order  $(M - 2)$  in  $(i\omega)$ :

$$a_{ik}(\omega) = \sum_{m=0}^{M-2} a_{(ik)m} (i\omega)^m \quad \forall i, k \quad (75)$$

$$\mathbf{A}(\omega) = \begin{pmatrix} i\omega + \beta_{10} + \beta_{12} & 0 & \dots & 0 & 0 \\ -\beta_{12} & i\omega + \beta_{23} & \dots & 0 & 0 \\ \vdots & \vdots & \ddots & \vdots & \vdots \\ 0 & 0 & \dots & i\omega + \beta_{(M-2)(M-1)} & 0 \\ 0 & 0 & \dots & -\beta_{(M-2)(M-1)} & i\omega + \beta_{(M-1)0} \end{pmatrix}, \quad (80)$$

with coefficients  $a_{(ik)m}$  which are functions of the constant rates  $\beta_{lm}$  only. Finally,

$$B_i^\delta(\omega) = b_{(i)} e^{-i\omega t} \quad \forall i, \quad (76)$$

where the  $b_{(i)}$  are functions of the constant rates  $\alpha_i$  and the time dependent fraction of channels in the open state  $c_0(t)$ . Taking together Eqs. (74) to (76), we obtain:

$$C_k(\omega) = \frac{\sum_{n=0}^{M-2} d_n (i\omega)^n e^{-i\omega t}}{\sum_{m=0}^{M-1} a_m (i\omega)^m} \sim \frac{1}{i\omega} e^{-i\omega t} \quad (77)$$

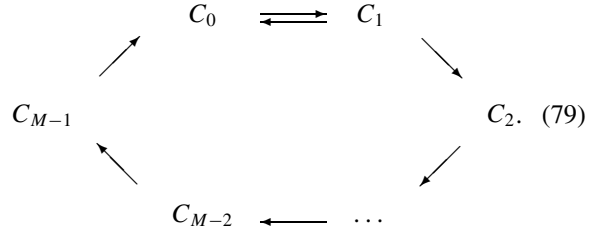
for  $k = 1, \dots, M - 1$  and some coefficients  $d_n$  which only depend on the constant rates  $\alpha_k$  and  $\beta_{ij}$  as well as  $c_0(t)$ . For the power spectral density  $P_{c_i}(\omega)$  we obtain:

$$P_{c_k}(\omega) = |C_k(\omega)|^2 \sim \frac{1}{\omega^2} \quad (78)$$

for  $k = 1, \dots, M - 1$  with  $C_k(\omega)$ , i.e.  $P_{c_k}(\omega)$  converges to zero like  $\omega^{-2}$  for  $\omega \rightarrow \infty$ .

Note that this general frequency dependence describes the slowest convergence. For specific models,  $P_{c_k}(\omega)$  may converge  $\sim \frac{1}{\omega^s}$  with  $s > 2$  for some  $k$ . In one of these specific models, the transition to the open state  $C_{M-1}$  occurs through a chain of intermediate nonconducting states  $C_1, \dots, C_{M-2}$  after transmitter binding

to  $C_0$ :



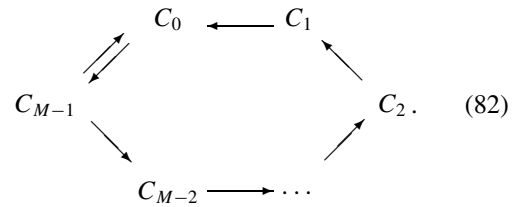
In this case,  $\mathbf{A}(\omega)$  takes a diagonal form with non-zero subdiagonal elements:

and

$$\mathbf{B}(\omega) = \sum_j e^{-i\omega t_j} c_0(t_j) \begin{pmatrix} \alpha \\ 0 \\ \vdots \\ 0 \end{pmatrix}. \quad (81)$$

Together with Eq. (73), we obtain for the PSD of the closed state  $C_{M-1}$  the  $\omega$ -dependence  $P_{C_{M-1}}(\omega) \sim \frac{1}{\omega^s}$  for  $\omega \rightarrow \infty$ .

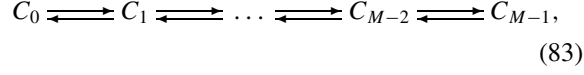
Another example is when the open state  $C_{M-1}$  is obtained by direct transmitter binding to the closed state  $C_0$ , while the transition between  $C_{M-1}$  and  $C_0$  can also occur via a chain of intermediate closed states  $C_1, \dots, C_{M-2}$ :



This particular scheme yields a diagonal form of  $\mathbf{A}(\omega)$  with non-zero superdiagonal elements. Here,  $P_{C_{M-1}}(\omega) \sim \frac{1}{\omega^2}$  for  $\omega \rightarrow \infty$ .

In the particular case of a linear transition diagram in which the closed state  $C_0$  and open state  $C_{M-1}$  are linked by a chain of intermediate closed states  $C_1, \dots,$

$C_{M-2}$



$\mathbf{A}(\omega)$  is tridiagonal and  $P_{C_{M-1}}(\omega) \sim \frac{1}{\omega^4}$  for  $\omega \rightarrow \infty$ .

### Appendix 3: Power Spectral Density of Pulse-Based Kinetic Model

Consider the two-state kinetic model of Eq. (1), but instead of describing the transmitter time course  $T$  as Dirac delta function as in Eq. (4), we use a ‘‘pulse-based kinetic model’’ (Destexhe et al., 1994), where  $T$  occurs as a brief pulse of amplitude  $T_{\max}$  and duration  $T_{\text{dur}}$ . The solution of this model is composed of two exponentials:

1. During a pulse ( $t_0 < t < t_1$ ),  $T = T_{\max}$  and  $c(t)$  is given by:

$$c(t - t_0) = c_\infty + (c(t_0) - c_\infty) \exp[-(t - t_0)/\tau_c] \quad (84)$$

where

$$c_\infty = \frac{\alpha T_{\max}}{\alpha T_{\max} + \beta}, \quad \tau_c = \frac{1}{\alpha T_{\max} + \beta}.$$

2. After a pulse ( $t > t_1$ ),  $T = 0$ , and  $c(t)$  is given by:

$$c(t - t_1) = c(t_1) \exp[-\beta (t - t_1)]. \quad (85)$$

The power spectral density  $P_c(\omega)$  of this 2-state kinetic model takes the form

$$P_c(\omega) = \frac{2\alpha^2 g_{\max}^2 T_{\max}^2}{C_3^2 \omega^2 ((C_3 \beta - \omega^2)^2 + \omega^2 (C_3 + \beta)^2)} \times (\beta^2 C_3^2 + \omega^2 (C_3^2 + D_1^2) + C_3 \beta \omega (C_3 - D_1)) \times \sin(\omega T_{\text{dur}}) - C_3 (\beta^2 C_3 + \omega^2 D_1) \cos(\omega T_{\text{dur}}),$$

where  $D_1 = \beta + (C_3 - \beta)e^{-T_{\text{dur}}C_3}$ . At high frequencies, the PSD shows oscillations (sin and cos terms above), which are caused by the discontinuity of the pulse in the time domain (as noted by Lowen and Teich, 1990). The asymptotic behavior is  $\omega^{-4}$  in this particular case. For low frequencies (typically below 500 Hz for the kinetics considered here), the power spectral density is

approximately Lorentzian, with a power spectral density given by

$$P_{\text{Lorentz}}(\omega) = \frac{2D\tau^2}{1 + \omega^2\tau^2}, \quad (86)$$

where

$$D = \frac{3E_1^2}{C_3^2 E_2}, \quad (87)$$

$$\tau^2 = \frac{E_2}{12\beta^2 C_3^2 E_1}, \quad (88)$$

denote the power and time constant of the Lorentzian, respectively, with

$$E_1 = C_3^2 + D_1^2 + (D_1 - C_3(1 + \beta T_{\text{dur}}))^2, \\ E_2 = C_3^3 \beta^2 T_{\text{dur}}^2 (C_3 \beta T_{\text{dur}}(4 + \beta T_{\text{dur}}) - 4D_1 \\ \times (3 + \beta T_{\text{dur}})) + 12(C_3^2 + \beta^2) E_1,$$

and

$$C_1 = \frac{g_{\max} \alpha T_{\max}}{\beta C_3^2} (\beta (T_{\text{dur}} C_3 + e^{-T_{\text{dur}} C_3} - 1) \\ + C_3 (1 - e^{-T_{\text{dur}} C_3})), \\ C_2 = \frac{g_{\max}^2 \alpha^2 T_{\max}^2}{2 \beta C_3^3} \\ \times (\beta (2T_{\text{dur}} C_3 + 4e^{-T_{\text{dur}} C_3} - e^{-2T_{\text{dur}} C_3} - 3) \\ + C_3 e^{-2T_{\text{dur}} C_3} (1 - e^{T_{\text{dur}} C_3})^2), \\ C_3 = \beta + \alpha T_{\max}.$$

## References

- Bernander Ö, Douglas RJ, Martin KAC, Koch C (1991) Synaptic background activity influences spatiotemporal integration in single pyramidal cells. *Proc. Natl. Acad. Sci. USA* 88: 11569–11573.
- Brunel N, Chance FS, Fourcaud N, Abbott LF (2001) Effects of synaptic noise and filtering on the frequency response of spiking neurons. *Phys. Rev. Lett.* 86: 2186–2189.
- Brunel N, Wang XJ (2001) Effects of neuromodulation in a cortical network model of object working memory dominated by recurrent inhibition. *J. Comput. Neurosci.* 11: 63–85.
- Campbell N (1909) The study of discontinuous phenomena. *Proc. Camb. Phil. Soc.* 15: 117–136.
- Chance FS, Abbott LF, Reyes AD (2002). Gain modulation from background synaptic input. *Neuron.* 35: 773–782.
- Clements JD (1996). Transmitter time course in the synaptic cleft: Its role into central synaptic function. *Trends Neurosci.* 19: 163–171.
- Cragg BG (1967) The density of synapses and neurones in the motor and visual areas of the cerebral cortex. *J. Anat.* 101: 639–654.

- Dayan P, Abbott LF (2001). *Theoretical Neuroscience*. MIT Press, Cambridge, MA.
- DeFelipe J, Fariñas I (1992) The pyramidal neuron of the cerebral cortex: Morphological and chemical characteristics of the synaptic inputs. *Prog. Neurobiol.* 39: 563–607.
- DeFelipe J, Alonso-Nanclares L, Arellano JI (2002) Microstructure of the neocortex: Comparative aspects. *J. Neurocytol.* 31: 299–316.
- Evarts EV (1964) Temporal patterns of discharge of pyramidal tract neurons during sleep and waking in the monkey. *J. Neurophysiol.* 27: 152–171.
- Destexhe A, Mainen ZF, Sejnowski TJ (1994) Synthesis of models for excitable membranes, synaptic transmission and neuromodulation using a common kinetic formalism. *J. Comput. Neurosci.* 1: 195–230.
- Destexhe A, Paré D (1999) Impact of network activity on the integrative properties of neocortical pyramidal neurons in vivo. *J. Neurophysiol.* 81: 1531–1547.
- Destexhe A, Rudolph M, Fellous J-M, Sejnowski TJ (2001) Fluctuating synaptic conductances recreate in-vivo—like activity in neocortical neurons. *Neuroscience* 107: 13–24.
- Doiron B, Longtin A, Berman N, Maler L (2000) Subtractive and divisible inhibition: Effect of voltage-dependent inhibitory conductances and noise. *Neural Comput.* 13: 227–248.
- Fellous J-M, Rudolph M, Destexhe A, Sejnowski TJ (2003) Synaptic background noise controls the input/output characteristics of single cells in an in vitro model of in vivo activity. *Neuroscience* 122: 811–829.
- Gerstner W, Kistler W (2002) *Spiking Neuron Models*. Cambridge University Press, Cambridge, UK.
- Hanson FB, Tuckwell HC (1983) Diffusion approximation for neuronal activity including reversal potentials. *J. Theor. Neurobiol.* 2: 127–153.
- Hines ML, Carnevale NT (1997) The NEURON simulation environment. *Neural Comput.* 9: 1179–1209.
- Johannesma PIM (1968) Diffusion models of the stochastic activity of neurons. In: Caianello ER (ed.), *Neural Networks*. Springer, Berlin, pp. 116–144.
- Koch C (1999) *Biophysics of Computation*. Oxford University Press, Oxford, UK.
- Lánský P, Lánská V (1987) Diffusion approximation of the neuronal model with synaptic reversal potentials. *Biol. Cybern.* 56: 19–26.
- Lánský P, Rodríguez R (1999) Two-compartment stochastic model of a neuron. *Physica D.* 132: 267–286.
- Lánský P, Rospars JP (1995) Ornstein-Uhlenbeck model neuron revisited. *Biol. Cybern.* 72: 397–406.
- Lowen SB and Teich MC (1990) Power-law shot noise. *IEEE Trans. Inform. Theory* 36: 1302–1318.
- Manwani A, Koch C (1999) Detecting and estimating signals in noisy cable structure, I: neuronal noise sources. *Neural Comput.* 11: 1797–1829.
- Matsumura M, Cope T, Fetz EE (1988) Sustained excitatory synaptic input to motor cortex neurons in awake animals revealed by intracellular recording of membrane potentials. *Exp. Brain Res.* 70: 463–469.
- Mattia M, Del Giudice P (2000) Efficient event-driven simulation of large networks of spiking neurons and dynamical synapses. *Neural Comput.* 12: 2305–2329.
- Papoulis A (1991) *Probability, Random Variables, and Stochastic Processes*. McGraw-Hill, Boston, MA.
- Prescott SA, De Koninck Y (2003) Gain control of firing rate by shunting inhibition: Roles of synaptic noise and dendritic saturation. *Proc. Natl. Acad. Sci. USA* 100: 2076–2081.
- Press WH, Flannery BP, Teukolsky SA, Vetterling WT (1986) *Numerical Recipes. The Art of Scientific Computing*. Cambridge University Press, Cambridge, MA.
- Rapp M, Yarom Y, Segev I (1992) The impact of parallel fiber background activity on the cable properties of cerebellar purkinje cells. *Neural Comput.* 4: 518–533.
- Ricciardi LM (1976) On the transformation of diffusion processes into the Wiener process. *J. Math. Analysis Appl.* 54: 185–199.
- Rudolph M, Destexhe A (2003a) A fast-conducting, stochastic integrative mode for neocortical dendrites in vivo. *J. Neurosci.* 23: 2466–2476.
- Rudolph M, Destexhe A (2003b) The discharge variability of neocortical neurons during high-conductance states. *Neuroscience* 119: 855–873.
- Rudolph M, Piwkowska Z, Badoual M, Bal T, Destexhe A (2004) A method to estimate synaptic conductances from membrane potential fluctuations. *J. Neurophysiol.* 91: 2884–2896.
- Steriade M (1978) Cortical long-axoned cells and putative interneurons during the sleep-waking cycle. *Behav. Brain Sci.* 3: 465–514.
- Steriade M, Timofeev I, Grenier F (2001) Natural waking and sleep states: A view from inside neocortical neurons. *J. Neurophysiol.* 85: 1969–1985.
- Szentagothai J (1965) The use of degeneration in the investigation of short neuronal connections. In: M Singer, JP Shade, (eds.) *Progress in Brain Research*, vol. 14. Elsevier Science Publishers, Amsterdam, pp. 1–32.
- Tiesinga PHE, José JV, Sejnowski TJ (2000) Comparison of current-driven and conductance-driven neocortical model neurons with Hodgkin-Huxley voltage-gated channels. *Phys. Rev. E* 62: 8413–8419.
- Tuckwell HC, Wan FYM, Rospars JP (2002) A spatial stochastic neuronal model with Ornstein-Uhlenbeck input current. *Biol. Cybern.* 86: 137–145.
- Uhlenbeck GE, Ornstein LS (1930). On the theory of the Brownian motion. *Phys. Rev.* 36: 823–841.
- van Rossum MCW (2001) The transient precision of integrate and fire neurons: Effect of background activity and noise. *J. Comput. Neurosci.* 10: 303–311.